Thermal and structural optimization of a small satellite using composite materials

Mariana Coelho dos Santos Moreira
mariana.moreira@tecnico.ulisboa.pt

Instituto Superior Técnico, Universidade de Lisboa, Portugal

December 2019

Abstract

The development of CubeSats equipped with new structural materials suggests a new alternative to the use of the conventional aluminium. A lighter structure capable of providing the structural and thermal performance required during the satellite's lifetime, would enable the increase of mass budget used in other subsystems. This paper describes the assessment of viable laminated composite materials as an alternative to the typical aluminium used in the side panels structure of a CEiiA's 3U CubeSat. Eighteen laminates are designed with distinct stacking sequences made of Carbon Fibre Reinforced Polymer (CFRP) or Glass Fibre Reinforced Polymer (GFRP) combined with laminae of aluminium, pyrolytic graphite or copper mesh. A decision matrix is devised in which composites with lightweight, good mechanical properties and high thermal conductivity are preferred. Three laminates are selected, composed by CFRP with an aluminium core, CFRP with pyrolytic core and GFRP with pyrolytic core. To evaluate the structural and thermal behaviour of the satellite with the laminate side panels, linear static, normal modes and static thermal FEM analyses are performed. If the satellite's behaviour is not similar to the one with the aluminium panels, an optimization design cycle is performed. The investigation revealed that hybrid laminates provide the structural and thermal performances required with a lower weight than the aluminium design. A 58.1% structural mass reduction on each panel is attained for the final optimized composite laminate, formed by laminae of CFRP with pyrolytic graphite core of 0.4 mm thickness and total thickness of 1.6 mm.
Keywords: CubeSats, laminated composite materials, hybrid laminates, structural finite element analyses, thermal finite element analyses, space environment.

1. Introduction

Modern society is highly dependent on space and considering that today's economy relies on the capacity of nations to develop knowledge, innovation and technology are a priority on their agendas [1].

Traditionally, the access to space was limited to governmental institutions, due to the high costs associated with the development of large and sophisticated spacecrafts. However, in the last decade, space industry set a trend to develop and launch smaller satellites, due to their lower production costs and development time, allowing private companies to enter the space market as well [2]. This growth of smaller missions was also driven by the advancements on miniaturized technology, which foster the development of increasingly sophisticated missions without the loss of performance, and the creation of CubeSat concept [2]. The advancements of technology and the optimization of CubeSats are, therefore, a first concern of space industry, providing small satellites with higher potential value in terms of scientific return and commercial revenue [2].

CubeSats have size and mass constraints, and a compromise between the structure and other subsystems and payloads is required to reach a cost effective design that will not jeopardize the satellite's mission.

In light of that compromise, the main purpose of this work is to assess the possibility to reduce the structural mass of a CEiiA's putative satellite without compromising its structural and thermal integrity. Hence, the challenge is to develop a solution that has a lower mass than the conventional aluminium alloy CubeSat's structures by replacing the satellites side panels with laminated composite materials. In order to evaluate the structural and thermal behaviour of the different satellite designs, linear static, normal modes and static thermal analyses were performed using a Finite Element Method (FEM), followed by structural and thermal optimization design cycles to meet the requirements sought.

In this paper, in Sec. 2 the methodology used to design and select the laminates to be assessed as viable alternatives to the aluminium is presented including the description of the optimization design cycle of the initial laminates.

In Sec. 3, the structural FEM models (linear static and normal mode) created based on the CAD model of the satellite, to evaluate the structural behaviour of the

different satellite designs, are described. The structural requirements and the simulations results for the structural optimization of the composite laminates are also presented.

Afterwards, the development of the thermal FEM model, the thermal requirements and the simulations results for the laminates thermal optimizations performed are presented in Sec. 4.

Finally, the final thermo-structural simulations results are presented for the optimized composite laminates and the discussion of the results obtained is provided in Sec. 5.

2. Composite Materials Design Methodology

It is important to remember that the main goal of this work is to assess the possibility of reducing the structural mass of a 3U CubeSat by replacing the 2 mm thickness aluminium side panels with a laminated composite material, without compromising the structural and thermal performance of the satellite. Hence, the satellite with laminated composite materials as their side panels must be lighter and present an identical structural and thermal behaviour as the aluminium one.

Therefore, an iterative process, in which each optimization step is characterized by a change in one of the parameters influencing the structural and/or thermal performance of the composite laminate is required. This process can be subdivided into two main parts: the preliminary selection approach and the optimization cycle.

Fig. 1 (a) shows the preliminary selection approach process, which main goal is to select the most promising laminated composite materials among several stacking schemes and lamina materials, thus narrowing the number of laminates to be optimized.

The starting point of this process was two unidirectional fibre reinforced polymer composites, CFRP and GFRP composite. For each composite material several laminate composite were built, in which laminae of aluminium, copper mesh or pyrolytic graphite were added to increase thermal conductivity of the laminate. Eighteen different laminated composite materials were created and a decision matrix to select the three most suitable laminates evaluated. In order to simplify the different stacks identification, a number was assigned to each of the plates designed. The materials with the three highest scores present a lamination scheme ($0^o/90^o$/Core/$90^o/0^o$) and with each fibre reinforced polymer (FRP) lamina 0.15 mm thick. These hybrid structures are the following:

1. Number 3: CFRP with aluminium core and total thickness of 0.75 mm;
2. Number 7: CFRP with pyrolytic graphite core and total thickness of 0.7 mm;
3. Number 16: GFRP with pyrolytic graphite core and total thickness of 0.7 mm,

which represented a structural mass reduction on each panel of 74.7%, 80.6% and 77.3%, respectively.

Once selected, the baseline laminated composite materials, an optimization design cycle was carried out.

In Fig. 1 (b), the optimization cycle conducted is presented. It consists of an assessment of the resulting design performance, via linear static, modal and static thermal analysis: if the laminate is admissible, meeting all requirements , the optimization cycle is dismissed, otherwise the material configuration and design are revised (in Fig. 1 (b) the sequential requirement assessments are represented by D1, D2 and D3). Secs. 3 and 4 are dedicated to the structural and thermal optimization design cycles, respectively.

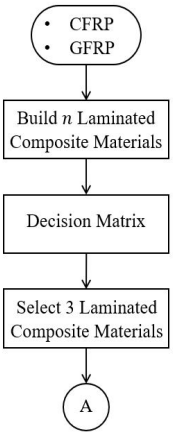

(a) Preliminary selection approach.

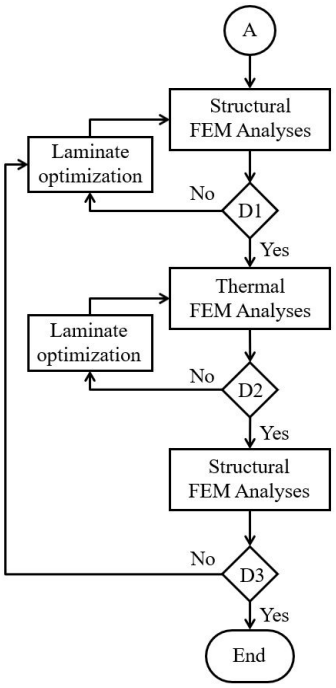

(b) Optimization design cycle.

Figure 1: Laminated composite materials' design methodology.

3. Structural Analysis

Following the establishment of the composite materials to be studied as an alternative for the aluminium side panels of a 3U CubeSat, the current section aims to present the structural optimizations performed. However, first the structural requirements that must be fulfilled by the spacecraft need to be defined.

3.1. Structural Requirements

According to the European Cooperation for Space Standardization (ECSS), satellite structures shall be designed to withstand the worst conditions predicted without compromising their structural integrity, thus allowing the mission to which it was designed to be successfully conducted [3]. The most structural demanding loads in the life-cycle of satellites occur during launch and, therefore, the requirements are directly related to the environment which the satellite is subjected to while being transported into orbit inside the launch vehicle. Hence, the definition of the loads applied to the satellite are determined by the launch vehicle to be used, in the present work by the VEGA launcher.

Regarding the static loads, six different case scenarios must be considered for analysis. However, first it is necessary to evaluate the typical CubeSat position within the VEGA launcher, since the loads are defined in each of the launcher axes. According to reference [4], 3U CubeSats are usually laid down horizontally within VEGA and, therefore, the longitudinal loads are applied in the lateral direction of the satellite. To simplify the identification of each case, Tab. 1 was devised.

Table 1: Linear static case analysis.

Cases	Launcher coordinate system	Satellite coordinate system	Load
A	$z-$direction	$x-$direction	$+10.5g$
B	$z-$direction	$x-$direction	$-14.5g$
C	$y-$direction	$y-$direction	$+3.00g$
D	$y-$direction	$y-$direction	$-3.00g$
E	$x-$direction	$z-$direction	$+3.00g$
F	$x-$direction	$z-$direction	$-3.00g$

In linear static analyses, structures subjected to a certain load environment are designed to allow the maximum stress to be less than its materials strengths by a sufficient margin, known as the margin of safety (MOS), so that unexpected conditions other than those predicted for use in the analysis are accounted for [5]. Then, in the present work, a structure is considered not to fail if its MOS is greater than zero [5]. For isotropic materials, the MOS can be computed as [6]

$$\text{MOS} = \frac{\sigma_{allowable}}{\sigma_{result} \times \text{FOSU}} - 1, \tag{1}$$

where the $\sigma_{allowable}$ corresponds to the ultimate strength of a given material, FOSU to the ultimate factor of safety (FOSU=2 [5]) and σ_{result} correspond to the highest analysis stress obtained. To compute the stresses obtained, the von Mises theory was used.

As for laminated composite materials, a structure is considered to fail if its failure index (FI) is equal or higher than one. In the present work, the Tsai-Hill failure criteria was used.

With respect to the dynamic behaviour of space structures, to prevent structural damage or failure, the fundamental frequency of the structure must be higher than 115 Hz, for VEGA launcher.

To ensure that the satellite will meet all the structural requirements, its behaviour must the predicted, thus the need to perform FEM analyses and build the FEM models.

3.2. Structural FEM Models

The structural FEM models consisted of concentrated masses, 2D and 1D elements. The model resulted from different structure idealizations: all screws were converted into 1D structures; all structures were converted into 2D surfaces, represented by its mid-surfaces; and the electronic subsystems and the payload were replaced by each component's centre of gravity, which were then connected to the structure by rigid elements.

Regarding the boundary conditions, for the linear static analysis, the six case scenarios presented in Tab. 1 were considered and for each the loads were defined as acceleration vectors for gravity loads, applied to each of the axes with the respective magnitude. Once the static loads were applied, the movement constraints were established. Typically, the satellite rails are the only structure of the satellite in contact with the deployer capsule, therefore the movement in each case was confined to the corresponding perpendicular axes [7].

As for the modal analysis case, free vibration conditions were modelled, i.e. no boundary conditions were applied to the model.

Figs. 2 (a) and (b) show the structural FEM model created, due to legibility purposes not all elements are identified and two different views are presented.

3.3. Structural Optimization Design Process

Once the structural FEM models are finished, the optimization design cycle previously presented in Sec. 2, in Fig. 1 (b), can be carried out. The optimization processes followed can be summarized as follows: the linear static and normal mode analyses results were obtained and if the satellite with the composite laminates presented an identical structural response to the aluminium one, the analysis proceeded to the thermal analysis. If not, the laminates were optimized until an identical response was obtained.

In the linear static analysis, three distinct assessments were made.

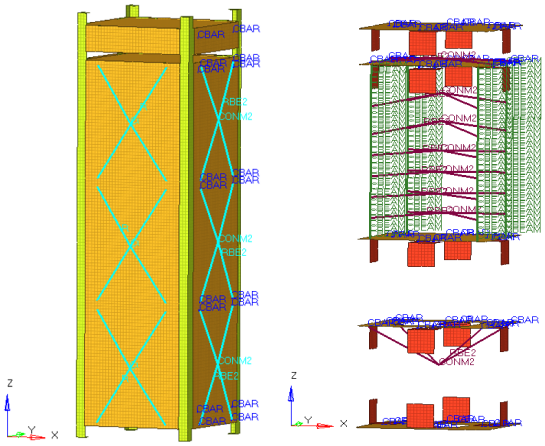

(a) External view. (b) Internal view.

Figure 2: External and internal views of the structural FEM model.

Firstly, the critical components, i.e. the components that presented the lowest MOS, in each design and load case were identified. Tab. 2 shows the critical MOS computed for each load case. For all cases a MOS$\geq$ 0 was attained and, therefore, the components did not fail, presenting a similar behaviour as the satellite with the aluminium panels.

Table 2: Critical components' MOS.

Cases	Aluminium	Laminate nº 3	Laminate nº 7	Laminate nº 16
A	3.000	3.300	3.450	3.280
B	1.930	2.110	2.220	2.090
C	14.19	15.32	15.55	15.20
D	14.18	15.32	15.53	15.14
E	29.18	18.10	17.92	17.46
F	29.00	18.13	17.93	17.50

Secondly, the FI of the satellite side panels, for each design, were computed. Tab. 3 presents the extreme failure indexes computed for each of the different materials. For all load cases, the laminated composite materials met the requirements established, i.e failure index smaller than 1.

Table 3: Maximum failure index of the satellite's side panels.

	Failure index		
Cases	Laminate nº 3	Laminate nº 7	Laminate nº 16
A	0.148	0.353	0.410
B	0.280	0.487	0.778
C	0.012	0.102	0.081
D	0.012	0.102	0.081
E	1.51E-03	0.029	0.011
F	6.94E-04	0.029	0.011

Finally, the bolts' MOS were computed. Once more, the structural requirement was met for all load cases.

As all the different designs presented a similar behaviour to the aluminium one, it was not necessary to optimize any of the proposed laminates and the normal mode analysis could be conducted.

The fundamental frequency of the satellite with 2 mm aluminium thickness plates was equal to 182.38 Hz, which meets the requirement of having a fundamental frequency higher than 115 Hz. However, none of the other laminate plates met this requirement and, therefore, their design needed to be revised. Hence, the thickness of CFRP or GFRP layers of each laminate were gradually increased, until they met the 115 Hz frequency goal. The laminates which met the requirement were:

- Number 3.1): CFRP with aluminium core and total thickness of 1.15 mm, each FRP lamina with 0.25 mm. With a structural mass reduction of 62.9% on each panel.
- Number 7.1): CFRP with pyrolytic graphite core and total thickness of 1.3 mm, each FRP lamina with 0.3 mm. Structural mass reduction of 62.9% on each panel.
- Number 16.1): GFRP with pyrolytic graphite core and total thickness of 1.7 mm, each FRP lamina with 0.4 mm. Structural mass reduction of 42.1% on each panel.

Tab. 4 shows the updated laminates fundamental frequencies, and, as stated before, all designs met the 115 Hz goal. Note that the first six frequencies are neglected, since they are associated with the rigid body motion due to the unconstrained model. Hence, the first four modes of vibration correspond to mode 7, 8, 9 and 10, being the fundamental frequency f_7.

Table 4: First natural frequencies of the structural optimized laminates.

Mode	Natural frequency [Hz]	Aluminium	Laminate nº 3.1)	Laminate nº 7.1)	Laminate nº 16.1)
1	f_1	9.24E-04	9.19E-04	1.26E-03	8.96E-04
2	f_2	7.35E-04	7.31E-04	9.19E-04	7.68E-04
3	f_3	5.22E-04	4.64E-04	4.47E-04	6.43E-04
4	f_4	3.96E-04	2.00E-04	3.90E-04	5.93E-04
5	f_5	1.85E-04	4.71E-04	4.26E-04	4.95E-04
6	f_6	5.65E-04	6.29E-04	7.43E-04	3.00E-04
7	f_7	182.28	122.69	137.26	118.70
8	f_8	182.47	124.69	139.72	120.79
9	f_9	190.71	125.80	140.41	121.98
10	f_{10}	208.11	178.53	180.34	163.57

Following these laminate optimizations, the thermal static analysis could be performed with the new suggested materials.

4. Thermal Analysis

The current section aims to provide a corresponding presentation to thermal analysis, as the one provided on the

last section for matters of structural nature.

4.1. Thermal Requirements

The requirements by the ECSS in Thermal Control General Requirements standard [8] state that the mission phases shall be represented by a coherent set of thermal design cases covering the extreme range of conditions experienced by the spacecraft. Therefore, the dimensioning environmental worst design cases must be used: the hot case, that represents the conditions that causes the highest temperatures in a satellite, i.e. maximum solar flux and electronic systems operating at full power; and the cold case, corresponding to eclipse conditions and with all electric components considered to be in a non-operational state with an idle power consumption.

The temperatures of all electric components must remain within the allowable temperatures defined by the systems' authority under such cases. Furthermore, temperature gradients must be specified and defined in accordance to the mission objectives and taking into account the spacecraft properties being analysed.

Tab. 5 shows the established hot and cold cases and the radiation fluxes reaching the satellite due to solar radiation G_S, albedo a_E and Earth's infrared radiation q_{IR}.

4.2. Thermal FEM Model

The thermal FEM model consisted in 3D, 2D and 1D elements, which resulted from different idealizations: all structures and electronic subsystems were converted into 2D structures, with the exception of the battery cells and magnetorquers, which were modelled as 3D structures with simplified geometries; the payload (nanocamera) was modelled as a 3D structure; and all screws were converted into 1D structures. Furthermore, radiative elements were assigned to each mesh element to account for the radiation exchanges.

In Figs. 3 (a) and (b), the thermal FEM model developed heretofore is presented, due to legibility purposes not all elements are identified.

4.3. Thermal Optimization Design Process

Once the thermal FEM model was completed, the thermal optimization design process could be conducted.

Table 5: Hot and cold case orbit and flux characteristics.

		Hot case	Cold case
Orbit type		SSO	
h	[km]	550	
e	[−]	0	
G_S [9]	[W/m^2]	1412.9	0
q_{IR} [9]	[W/m^2]	230	230
a_E [9]	[−]	0.3	0

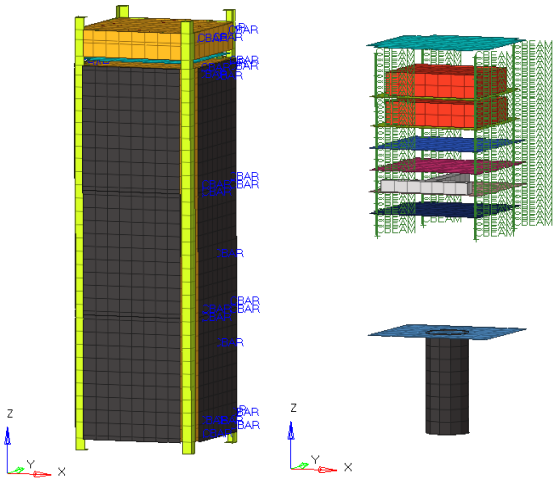

(a) External view. (b) Internal view.

Figure 3: External and internal views of the thermal FEM model.

To conduct the thermal optimization design process, an analogous procedure to the one used in the structural optimizations was applied: the static thermal analyses were conducted for the two worst cases defined in Sec. 4.1. If the laminated composite materials designs presented, at the very least, the same number of components complying with their operational temperatures as the aluminium one, the cycle was dismissed, if not the laminates were revised and updated. Additionally, the composite material panels shall have a temperature gradient similar to that of the aluminium ones.

Firstly the thermal behaviour of the aluminium design was discovered. In Fig. 4, the hot and cold cases minimum and maximum temperatures and the temperature gradients of each satellite component can be observed for the aluminium design. The components' operating temperature ranges are also presented. According to the results, for the hot case the transceiver exceeds its maximum operational temperature and the nanocamera its minimum operational temperature. In the cold case several components have a minimum temperature that falls below their minimum operating temperature.

Regarding, the laminate composite designs 3.1), 7.1) and 16.1), two distinct analyses were performed: in the first analysis the laminated composite materials were considered to have an equal absorptivity and emissivity as the aluminium, $\alpha = 0.14$ and $\varepsilon = 0.84$. Whereas, in the second analysis, the respective FRP absorptivity and emissivity mean values were used: for CFRP $\alpha = 0.8$ and $\varepsilon = 0.7$; for GFRP $\alpha = 0.3$ and $\varepsilon = 0.85$.

In the first analysis ($\alpha = 0.14$), the components that exceed their operational temperatures are the same as in the aluminium design for both extreme cases, hot and cold. Whereas, in the second analysis ($\alpha = 0.8$), the components' temperature of laminate designs n^o 3.1)

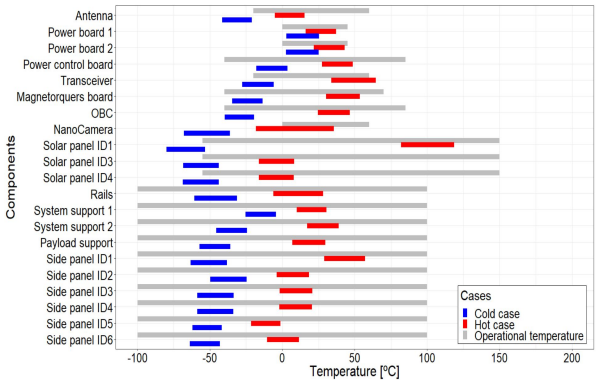

Figure 4: Operating ranges, minimum and maximum temperatures and temperature variation in each component for the aluminium design.

and 7.1) suffers drastic changes when compared with the aluminium design, specially in the hot case. Regarding, the laminate nº 16.1) an increase in its temperature is also observed and even though the increase is smaller, three components do not comply with their operational requirements. As for the cold case, similar temperatures are achieved in all laminate designs.

To better assess the effect of the side panels thermo-optical properties on the components temperatures Figs. 5, 6 and 7 were created. In these figures, the minimum and maximum temperatures achieved by the structure side panel ID1 and by the antenna in function of the absorptivity of the panels for the laminates nº 3.1), 7.1) and 16.1) are presented. The minimum and maximum temperatures for the aluminium design are also presented. Due to legibility reasons, only the temperatures of the side panel with ID1 and the antenna temperatures are depicted. However, it must be noted that the same behaviour in function of the absorptivity is achieved for all the other electronic components and structures.

From the figures, it can be clearly concluded that the absorptivity of the panels dictate the temperatures achieved by the components. The increase in the materials' absorptivity leads to an increase in the components temperature, therefore the temperatures achieved by the laminates with $\alpha = 0.8$ (nº 3.1) and 7.1)) are higher, than the laminate with $\alpha = 0.3$ (nº 16.1)).

For all laminates, the increase in temperatures is higher in the hot case, than in the cold case.

Since the influence of the thermo-optical properties on the satellite temperatures is already known, the respective FRP absorptivity values will be considered for the following analysis (CFRP $\alpha = 0.8$, GFRP $\alpha = 0.3$).

Regarding the thermal gradients requirement, all laminates did not meet the requirement, presenting higher thermal gradients. Hence, the laminate designs needed to be revised. The laminates which met the thermal gradient requirements were the following hybrid structures:

- Number 3.3): CFRP with aluminium core of 1.7 mm thickness and total thickness of 2.7 mm. Each FRP lamina with 0.25 mm. Increase of 14.6% of structural mass on each panel;
- Number 7.3): CFRP with pyrolytic graphite core of 0.4 mm thickness and total thickness of 1.6 mm. Each FRP lamina with 0.3 mm. Structural mass reduction of 58.1% on each panel;
- Number 16.3): GFRP with pyrolytic graphite core of 0.5 mm thickness and total thickness of 2.1 mm. Each FRP lamina with 0.4 mm. Structural mass reduction of 35.8% on each panel.

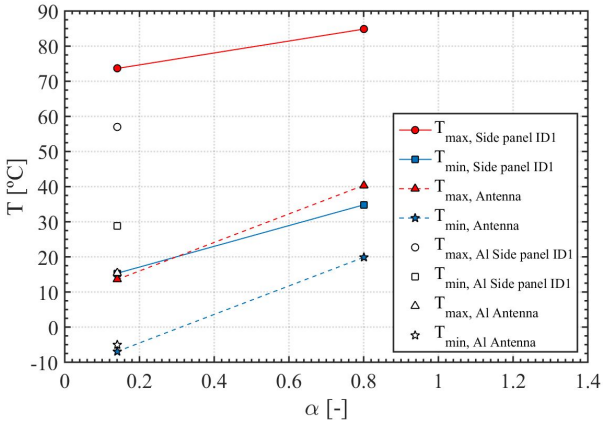

(a) Hot case.

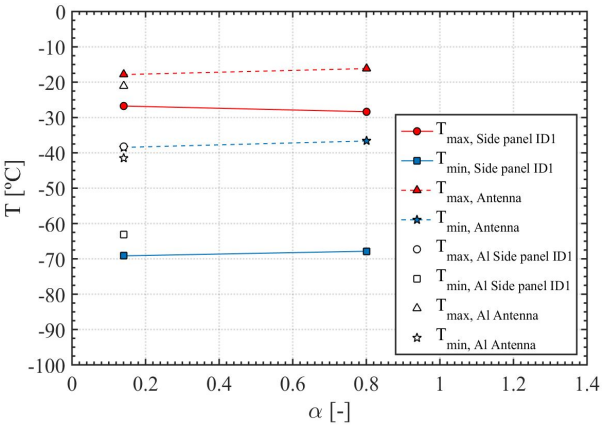

(b) Cold case.

Figure 5: Maximum and minimum temperatures in function of the panels' absorptivity for laminate nº 3.1) design.

Although, the thermal gradient requirement was met by all three, a 14.5% increase in the structural mass on each panel was obtained for laminate nº 3.3). Therefore, only laminate nº 7.3) and 16.3) were valid candidates.

Up until this point, the influence of the thermal-optical properties on the satellite components was assessed and the thermal gradient requirement was met by the valid candidates. However, with these new laminates, it was necessary to evaluate the effect of the in-

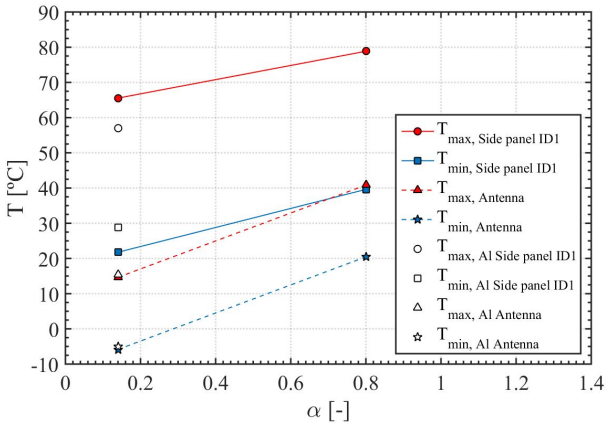

(a) Hot case.

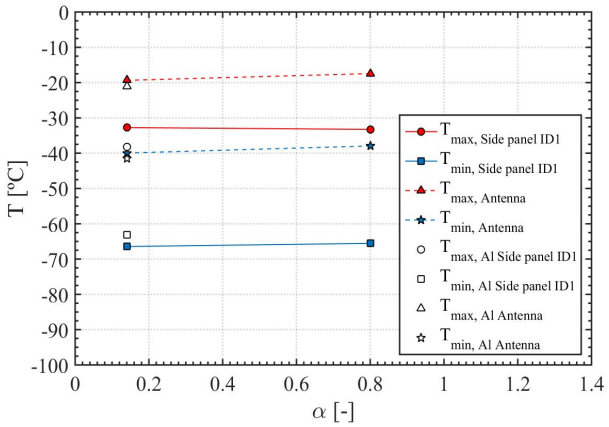

(b) Cold case.

Figure 6: Maximum and minimum temperatures in function of the panels' absorptivity for laminate nº 7.1) design.

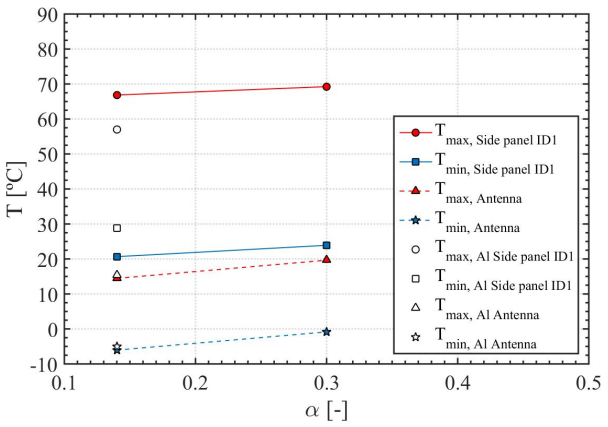

(a) Hot case.

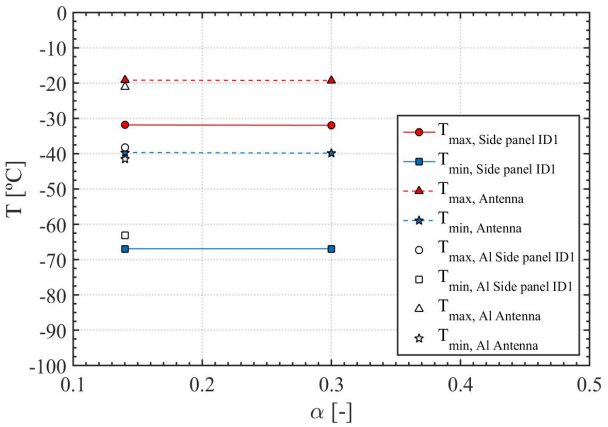

(b) Cold case.

Figure 7: Maximum and minimum temperatures in function of the panels' absorptivity for laminate nº 16.1) design.

crease of thermal conductivity on the structure's side panels and components temperature.

In Figs. 8 and 9, the maximum and minimum temperature achieved by the side panels and components in function of the laminates thermal conductivity are presented. Due to legibility reasons, only the temperatures of the side panel with ID1 and the antenna temperatures are depicted.

It can be concluded that the antenna temperature changes slightly with the increase of the panels' thermal conductivity for the hot and cold cases, with a maximum of 2 ºC. Whereas for the side panels a change up to approximately 10 ºC is reached and, the maximum and minimum structure temperatures tend to decrease their difference in both cases, i.e. decreasing the thermal gradient.

From the figures it can also be clearly seen the difference between the temperatures of the aluminium design and the laminate designs. As previously observed, in the hot case the laminates present higher mean values than the aluminium, due to their higher absorptivity value, whereas in the cold case the difference between the designs is almost null.

Taken into account all the analyses performed, it can be said that, for the satellite being studied, the thermal conductivity of the side panels does not influence the temperature of its components. The main responsible for the components' temperature, is the panels absorptivity. In order to meet the thermal requirements, a coat of paint with a similar absorptivity as the aluminium can be added to the laminate.

Following the thermal analysis, the linear static and normal mode analysis were conducted for the updated laminates, to ensure they meet the structural requirements as well.

5. Thermo-Structural Analysis Results and Discussion

In the current section the optimization design cycle is finalized: the static linear and normal mode analysis are performed for the updated composite laminates and the thermal results obtained are recalled. A discussion on

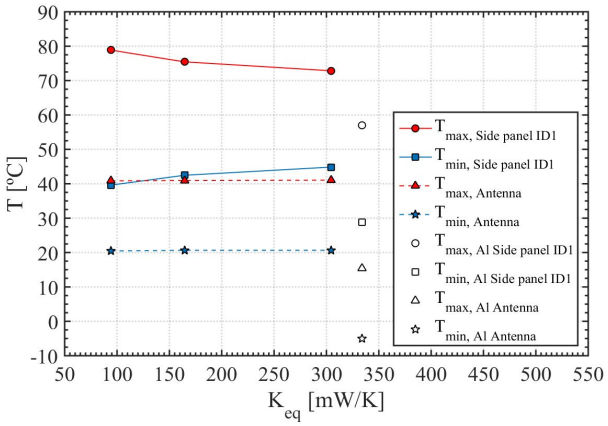

(a) Hot case.

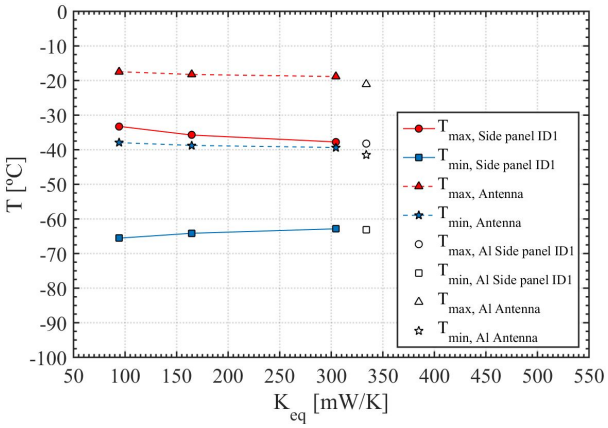

(b) Cold case.

Figure 8: Maximum and minimum temperatures in function of the panels' thermal conductivity for laminates with CFRP and pyrolytic graphite core design.

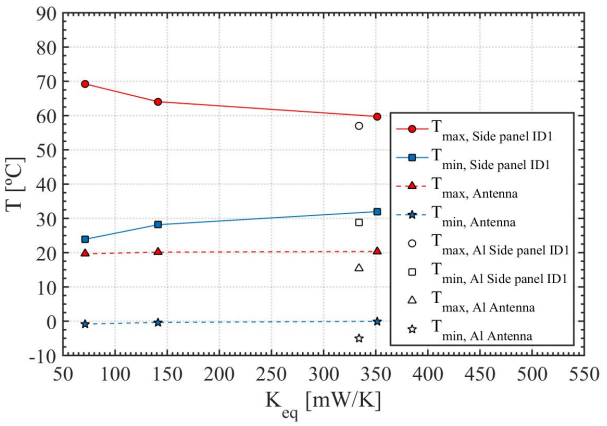

(a) Hot case.

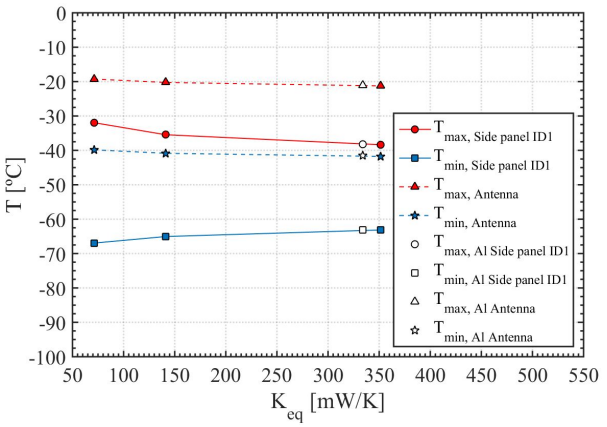

(b) Cold case.

Figure 9: Maximum and minimum temperatures in function of the panels' thermal conductivity for laminates with GFRP and pyrolytic graphite core design.

the final results obtained is also performed.

In Tab. 6 the computed MOS for the critical components in each load case are presented, for all cases the structural requirement MOS≥ 0 was met.

Regarding the side panels, the extreme failure indexes computed for each of the new materials are presented in Tab. 7. The composite laminates requirements, i.e failure index smaller than 1, was attained for all load cases.

One last assessment was made concerning the bolts' MOS: the full extension of designs met the requirement MOS≥ 0.

All the requirements regarding the linear static analysis were met, hence normal mode analyses were conducted for these two laminates. Tab. 8 shows the updated laminates fundamental frequencies, and, as can be seen, all designs also met the 115 Hz goal.

Since, the new laminates presented an identical structural behaviour to the aluminium panel design, the laminates do not need to be revised. Hence, the thermal analysis did not need to be conducted again, being the results obtained in Sec. 4 maintained for these laminates.

Recalling the thermal results, both materials did not comply with the requirements, i.e. presenting an identical response as the aluminium design. Therefore, for an operating mode, a coat of paint with an identical absorptivity as the aluminium can be added to the laminates so that similar temperatures could be attained.

Nevertheless, although the manufacturers did not present the components' survival temperature ranges, from state of the art evaluations performed it could be concluded that most components present a survival temperature range of -55 °C to 120 °C. Therefore, in all designs previously presented, for a non operating mode, all components would survive in the hot case and only the solar panels and nanocamera would not in the cold case.

So far, both laminates presented a similar structural and thermal behaviour. However, laminate n^o 7.3) allowed a further 22.3% and 58.1% reduction of structural mass, when compared with the laminate n^{o}16.3) and with the aluminium design, respectively. There-

Table 6: Updated critical components' MOS.

Cases	Aluminium	Laminate nº 7.3)	Laminate nº 16.3)
A	3.000	3.290	3.190
B	1.930	2.100	2.030
C	14.19	15.05	14.58
D	14.18	15.04	14.57
E	29.18	23.60	22.62
F	29.00	23.56	22.62
Component		System Support	

Table 7: Updated maximum failure index of the satellite's side panels.

	Failure index	
Cases	Laminate nº 7.3)	Laminate nº 16.3)
A	0.239	0.188
B	0.329	0.258
C	0.069	0.054
D	0.069	0.055
E	0.063	0.044
F	0.063	0.044

fore, since the main goal of this work was to reduce the structural mass of the satellite, the CFRP with pyrolytic graphite core of 0.4 mm thickness and total thickness of 1.6 mm was the laminated composite material selected between the two.

Even though, a coat of paint must be added to this laminate, a structural mass reduction of 58.1% on each panel is a big improvement relatively to the aluminium design. It can be concluded that laminates can offer big reductions of the structural mass without compromising the structural and thermal performance of the satellite. However, it must be noted that only by inserting a high thermal conductivity core within the FRP it is possible to achieve all the thermal conductivity requirements.

In Figs. 10, 11 and 12, the MOS and failure indexes, the normal modes and the thermal results for the final optimized laminate can be observed. Note that, MOS values greater than 6 were represented as equal to 6.

6. Conclusions

The main goal of this work was to assess if laminated composite materials could be a viable alternative to the typical aluminium side panels of a CEiiA's 3U CubeSat, with the purpose of reducing the structural mass of the satellite, without loss of structural and thermal performance.

In order to accomplish that goal, three composite laminates were selected among 18 hybrid laminates with laminae of CFRP or GFRP and laminae of aluminium, pyrolytic graphite or copper mesh, with distinct stacking schemes. The selected laminates were: CFRP with aluminium core and total thickness of 0.75 mm; CFRP with pyrolytic graphite core and total thickness of 0.7 mm; and GFRP with pyrolytic graphite core and total thickness of 0.7 mm, which represented a structural mass reduction of 74.7%, 80.6% and 77.3% on each panel, respectively.

Once selected the laminated composite materials, linear static, normal mode and thermal analyses were carried out. The respective FEM models were created and the simulations conducted, with the previous laminated

Table 8: First natural frequencies of the thermal optimized laminates.

Mode	Natural frequency [Hz]	Aluminium	Laminate nº 7.3)	Laminate nº 16.3)
1	f_1	9.24E-04	8.61E-04	9.59E-04
2	f_2	7.35E-04	6.95E-04	5.23E-04
3	f_3	5.22E-04	4.95E-04	2.11E-04
4	f_4	3.96E-04	5.01E-04	8.29E-05
5	f_5	1.85E-04	6.16E-04	5.63E-04
6	f_6	5.65E-04	8.61E-04	6.05E-04
7	f_7	182.28	185.77	167.80
8	f_8	182.47	186.74	169.38
9	f_9	190.71	189.00	171.52
10	f_{10}	208.11	198.72	181.34

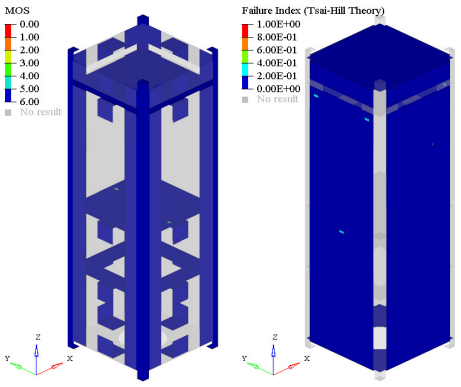

Figure 10: MOS and failure index FEM results of laminate nº 7.3) design for load case B.

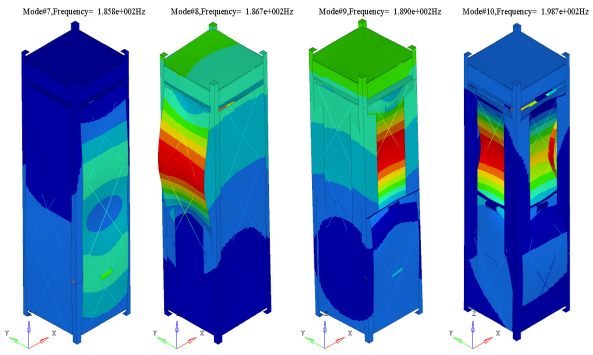

Figure 11: First four vibration modes of laminate nº 7.3) design.

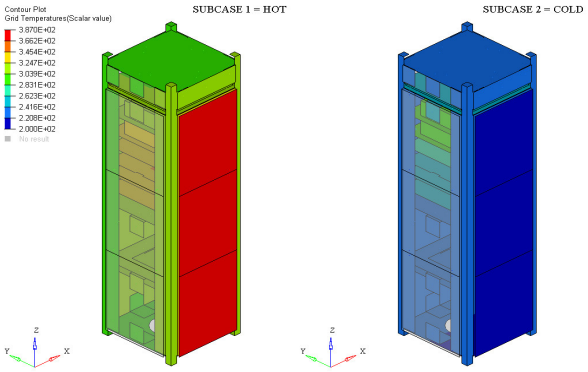

Figure 12: Hot and cold case temperature thermal analysis results for laminate n^{o} 7.3) design (units in Kelvin).

composite materials as their side panels. An optimization cycle was followed. The initially proposed laminates did not attain the required structural and thermal behaviour, therefore optimized laminated composite materials had to be created until the requirements were met.

Among the laminates that met all requirements, one of them was excluded as a valid candidate, since it represented a 14.6% increase in structural weight. The new optimized laminates were: CFRP with pyrolytic graphite core of 0.4 mm thickness and total thickness of 1.6 mm and each FRP lamina with 0.3 mm; and GFRP with pyrolytic graphite core of 0.5 mm thickness and total thickness of 2.1 mm and each FRP lamina with 0.4 mm.

From these laminates a distinction between the effect of the thermal conductivity of the panels and its absorptivity values on the component's temperature was identified. The results showed that the absorptivity of the panels dictates the components' temperature, whereas the thermal conductivity determines the thermal gradients of the panels. Therefore, only by adding a coat of paint with a proper absorptivity to the previous laminates, the components temperatures of the satellite studied can be adjusted.

Taking all this into account, it was concluded that hybrid structures can offer a viable alternative to the usual aluminium design, with major advantages as far as structural weight is concerned. However, since the main goal of this work was to reduce the satellites structural mass, the laminate which presented the higher structural mass reduction was selected as the final optimized solution. This laminate was the CFRP with pyrolytic graphite core of 0.4 mm thickness and total thickness of 1.6 mm, allowing a 58.1% of structural mass reduction on each panel.

7. Future work

The next step in this work would be to perform structural and thermal transient analyses, so that the behaviour of the laminated composite materials to transient loads could be analysed.

Since this work was a preliminary study on composite materials, their thermal expansion was not taken into account, therefore, in future analysis it must be a property that should be analysed and their effect on the structural behaviour of the satellite studied.

Another aspect that was not included in the preliminary analysis was the conductive links between the components, which were considered as perfect. Experimental studies must be performed so that the conductance behaviour between components could be determined.

The properties of the laminated composite materials should also be experimentally assessed, since some of its properties were computed using mathematical methods and others based on information available on literature. Additionally, other composite materials could be studied as possible solutions.

References

[1] B. Battrick et al. The impact of space activities upon society. *The European Space Agency, The International Academy of Astronautics, no. 237, ESA Publications Division - ESTEC*, 2015.

[2] Armen Poghosyan and Alessandro Golkar. CubeSat evolution: Analyzing CubeSat capabilities for conducting science missions. *Progress in Aerospace Sciences*, 88:59–83, January 2017.

[3] Space enginerering: Spacecraft mechanical loads analysis handbook. ECSS Secretariat, 2013. Document version ECSS-E-HB-32-26A.

[4] User manual for small spacecraft mission service proof of concept flight on vega. *Arianespace, ESA, Issue 1 Revision 0*, 2017.

[5] Space engineering: Structural factors of safety for spaceflight hardware. ECSS Secretariat, 2009. Document version ECSS-E-ST-32-10C.

[6] Space engineering: Threaded fasteners handbook. ECSS Secreatariat, 2010. Document version ECSS-E-HB-32-23A.

[7] A. Mehrparvar, D. Pignatelli, J. Carnahan, R. Munakar, W. Lan, A. Toorian, A. Hurputanasin, and S. Lee. Nanoracks cubesat deployer (NRCSD) interface control document. Technical report, 2015.

[8] Space engineering: Thermal control general requirements. ECSS Secretariat, 2015. Document version ECSS-E-ST-31C.

[9] Space engineering: Space environment. ECSS Secretariat, 2008. Document version ECSS-E-ST-10-04C.